PROCEEDINGS OF SCIENCE

Relevant Gluonic Momentum for Confinement and Gauge-Invariant Formalism with Dirac-mode Expansion

Hideo Suganuma[*], **Shinya Gongyo, Takumi Iritani**
Department of Physics, Kyoto University, Kitashirakawaoiwake, Sakyo, Kyoto 606-8502, Japan
E-mail: suganuma@scphys.kyoto-u.ac.jp

Arata Yamamoto

Department of Physics, The University of Tokyo, Tokyo 113-0033, Japan

We investigate the relevant gluon-momentum region for confinement in lattice QCD on 16^4 at β=5.7, 5.8 and 6.0, based on the Fourier expansion. We find that the string tension σ, i.e., the confining force, is almost unchanged even after removing the high-momentum gluon component above 1.5GeV in the Landau gauge. In fact, the confinement property originates from the low-momentum gluon component below 1.5GeV, which is the upper limit to contribute to σ. In the relevant region, smaller gluon momentum component is more important for confinement. Next, we develop a manifestly gauge-covariant expansion of the QCD operator such as the Wilson loop, using the eigen-mode of the QCD Dirac operator $\not{D} = \gamma^\mu D^\mu$. With this method, we perform a direct analysis of the correlation between confinement and chiral symmetry breaking in lattice QCD on 6^4 at β=5.6. As a remarkable fact, the confinement force is almost unchanged even after removing the low-lying Dirac modes, which are responsible to chiral symmetry breaking. This indicates that one-to-one correspondence does not hold for between confinement and chiral symmetry breaking in QCD.

International Workshop on QCD Green's Functions, Confinement and Phenomenology
5-9 September 2011
Trento, Italy

[*]Speaker.

PoS(QCD-TNT-II)044

1. Introduction

Nowadays, quantum chromodynamics (QCD) has been established as the fundamental gauge theory of the strong interaction. However, nonperturbative properties of low-energy QCD such as color confinement and chiral symmetry breaking [1] are not yet well understood, which gives one of the most difficult problems in theoretical physics. The nonperturbative QCD has been studied in lattice QCD [2, 3, 4] and various analytical frameworks [5, 6, 7, 8, 9, 10, 11].

In this paper, using lattice QCD, we research for the origin of color confinement in terms of the relevant gluon-momentum component based on the Fourier expansion in the Landau gauge [12]. We also investigate the correspondence between color confinement and chiral symmetry breaking using the Dirac-mode expansion in a gauge-invariant manner.

2. Relevant Region of Gluonic Momentum for Color Confinement

Many theoretical physicists consider that confinement phenomenon is brought by low-energy region of QCD, because of the strong QCD coupling in the infrared (IR) region. However, at the quantitative level, it is difficult to state the "relevant energy region" for confinement directly from QCD. Since nonperturbative phenomena are mainly brought by gluon dynamics, the key question here is *"what is the relevant gluon-momentum region responsible for confinement?"*

In this section, to get the answer, we study quantitative lattice-QCD analysis for the relevant gluon-momentum region for color confinement [12], based on the Fourier expansion of the link-variable. Our method consists of the following five steps.

Step 1. Generation of link-variable in the Landau gauge

We generate a gauge configuration on a L^4 lattice with the lattice spacing a by the lattice-QCD Monte Carlo method under space-time periodic boundary conditions. Here, we consider the link-variable $U_\mu(x) = e^{iagA_\mu(x)}$ fixed in the Landau gauge, where the fluctuation from gauge degrees of freedom is strongly suppressed, owing to the global suppression of gluon-field fluctuations [13].

Step 2. Four-dimensional discrete Fourier transformation

By the discrete Fourier transformation, we define the "momentum-space link-variable",

$$\tilde{U}_\mu(p) = \frac{1}{N_{\rm site}} \sum_x U_\mu(x) \exp(i\textstyle\sum_\nu p_\nu x_\nu), \tag{2.1}$$

with the lattice-site number $N_{\rm site}$. The momentum-space lattice spacing is given by $a_p \equiv 2\pi/(La)$.

Step 3. Imposing a cut in the momentum space

We impose a cut on $\tilde{U}_\mu(p)$ in the momentum space, as shown in Fig.1. Outside the cut, we replace $\tilde{U}_\mu(p)$ by the free-field link-variable, $\tilde{U}_\mu^{\rm free}(p) = \frac{1}{N_{\rm site}} \sum_x \exp(i\sum_\nu p_\nu x_\nu) = \delta_{p0}$, corresponding to $U_\mu(x) = 1$. Then, the momentum-space link-variable $\tilde{U}_\mu^\Lambda(p)$ with the cut is defined as

$$\tilde{U}_\mu^\Lambda(p) = \begin{cases} \tilde{U}_\mu(p) & (\text{inside cut}) \\ \tilde{U}_\mu^{\rm free}(p) = \delta_{p0} & (\text{outside cut}). \end{cases} \tag{2.2}$$

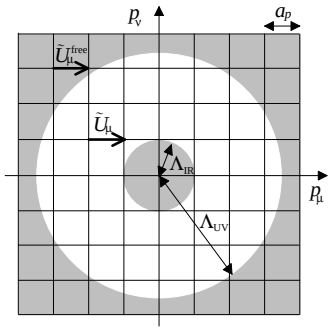

Figure 1: A schematic figure of the UV cut $\Lambda_{\rm UV}$ and the IR cut $\Lambda_{\rm IR}$ on momentum-space lattice, with the lattice spacing $a_p \equiv 2\pi/(La)$. The momentum-space link-variable $\tilde{U}_\mu(p)$ is replaced by the free-field link-variable $\tilde{U}_\mu^{\rm free}(p) = \delta_{p0}$ in the shaded cut regions.

Step 4. Inverse Fourier transformation

To return to the coordinate space, we carry out the inverse Fourier transformation as

$$U'_\mu(x) = \sum_p \tilde{U}^\Lambda_\mu(p) \exp(-i\textstyle\sum_\nu p_\nu x_\nu). \tag{2.3}$$

Since this $U'_\mu(x)$ is not an SU(3) matrix, we project it onto an SU(3) element $U^\Lambda_\mu(x)$ by maximizing ReTr$[U^\Lambda_\mu(x)^\dagger U'_\mu(x)]$. Such a projection is often used in lattice QCD algorithms. By this projection, we obtain the coordinate-space link-variable $U^\Lambda_\mu(x)$ with the cut, which is an SU(3) matrix and has the maximal overlap to $U'_\mu(x)$.

Step 5. Calculation of physical quantities

Using the cut link-variable $U^\Lambda_\mu(x)$, instead of $U_\mu(x)$, we calculate physical quantities as the expectation value in the same way as original lattice QCD.

With this method in lattice-QCD framework, we quantitatively determine the relevant energy scale of color confinement, through the analyses of the $Q\bar{Q}$ potential. The lattice QCD Monte Carlo simulations are performed on 16^4 lattice at β=5.7, 5.8 and 6.0 at the quenched level [12].

Figure 2 (a) and (b) show the $Q\bar{Q}$ potential $V(R)$ with the IR cutoff $\Lambda_{\rm IR}$ and the UV cutoff $\Lambda_{\rm UV}$, respectively. We get the following lattice-QCD results on the role of gluon momentum components.

- By the IR cutoff $\Lambda_{\rm IR}$, as shown in Fig.2(a), the Coulomb potential seems to be unchanged, but the confinement potential is largely reduced [12].
- By the UV cutoff $\Lambda_{\rm UV}$, as shown in Fig.2(b), the Coulomb potential is largely reduced, but the confinement potential is almost unchanged [12].

Figure 3 shows the $\Lambda_{\rm IR}/\Lambda_{\rm UV}$-dependence of the string tension σ obtained from the asymptotic slope of the $Q\bar{Q}$ potential $V(R)$ with the IR/UV cutoff. Note that the ordinary QCD system without the cutoff corresponds to $\Lambda_{\rm IR} = 0$ and $\Lambda_{\rm UV} = +\infty$. As shown in Fig.3(a), the string tension is significantly reduced by the IR-cutoff $\Lambda_{\rm IR}$ even for small values of $\Lambda_{\rm IR}$, and smaller gluon-momentum component seems to be more important for confinement.

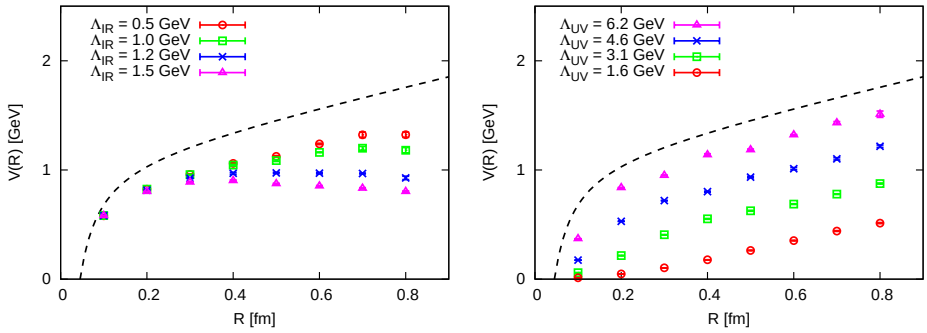

Figure 2: (a) The $Q\bar{Q}$ potential $V(R)$ with the IR cut $\Lambda_{\rm IR}$ plotted against the inter-quark distance R. (b) The $Q\bar{Q}$ potential with the UV cut $\Lambda_{\rm UV}$. Lattice QCD calculations are done on 16^4 lattice with $\beta = 6.0$, *i.e.*, $a \simeq 0.10$fm and $a_p \equiv 2\pi/(La) \simeq 0.77$GeV [12]. The dashed line is the original $Q\bar{Q}$ potential in lattice QCD.

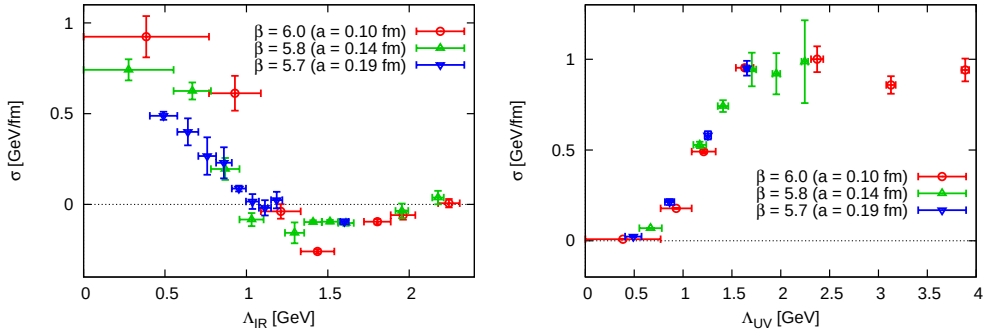

Figure 3: (a) The $\Lambda_{\rm IR}$-dependence and (b) the $\Lambda_{\rm UV}$-dependence of the string tension σ. The string tension is obtained from the asymptotic slope of the $Q\bar{Q}$ potential $V(R)$ with the IR/UV cutoff in lattice QCD on 16^4 at β =5.7, 5.8 and 6.0 [12]. The horizontal error-bar denotes the range from the discrete momentum, while the vertical error-bar is the statistical one. The broken line denotes the original value of $\sigma \simeq 0.89$GeV/fm.

As a remarkable fact, the string tension is almost unchanged even after cutting off the high-momentum gluon component above 1.5GeV, as shown in Fig.3(b) [12]. In fact, the confinement property originates from the low-momentum gluon component below 1.5GeV, which is the upper limit to contribute to σ. Note here that the relevant region $|p| \leq 1.5$GeV for the confinement is only a small part of the total four-dimensional Brillouin zone of the gluon field, $-\pi/a < p_\mu \leq \pi/a$ (μ=1,2,3,4). For example, at $\beta = 6.0$ (i.e., $a \simeq 0.1$fm), the relevant region $|p| \leq 1.5$GeV is less than 0.2% in the total Brillouin zone, as shown in Fig.4.

With the same method, we find also the relevant role of low-momentum gluons to chiral symmetry breaking in lattice QCD [14]. However, the response pattern against the cut is rather different from that on confinement, and higher-momentum gluons also contribute to the chiral condensate.

3. Gauge-Invariant Formalism with Dirac-mode Expansion: A Direct Investigation of Correlation between Confinement and Chiral Symmetry Breaking

Next, we newly develop a manifestly gauge-covariant expansion of the QCD operator such as the Wilson loop, using the eigen-mode of the QCD Dirac operator $\not{D} = \gamma^\mu D^\mu$, and investigate the relation between confinement and chiral symmetry breaking.

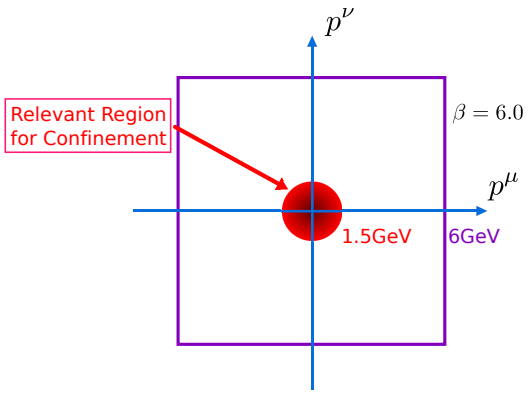

Figure 4: The relevant gluon-momentum region $|p| \leq 1.5$GeV for confinement in the Brillouin zone (BZ) $-\pi/a < p_\mu \leq \pi/a (\simeq 6\text{GeV})$ at $\beta = 6.0$. The relevant region is less than 0.2% in the four-dimensional BZ. In the relevant region, smaller gluon-momentum component is more important for confinement.

3.1 Gauge Covariant Expansion in QCD instead of Fourier Expansion

The previous method is based on the Fourier expansion, i.e., the eigen-mode expansion of the momentum operator p^μ. Because of the commutable nature of $[p^\mu, p^\nu] = 0$, all the momentum p^μ can be simultaneously diagonalized. which is one of the strong merits of the Fourier expansion. Also it keeps Lorentz covariance.

However, the Fourier expansion does *not* keep gauge invariance in gauge theories. Therefore, for the use of the Fourier expansion in QCD, one has to select a suitable gauge such as the Landau gauge, where the gauge-field fluctuation is strongly suppressed in Euclidean QCD.

As a next challenge, we consider a gauge-invariant method, using a gauge-covariant expansion in QCD instead of the Fourier expansion. In fact, we consider a generalization of the Fourier expansion or an alternative expansion with keeping the gauge symmetry.

A straight generalization is to use the covariant derivative operator D^μ instead of the derivative operator ∂^μ. However, due to the non-commutable nature of $[D^\mu, D^\nu] \neq 0$, one cannot diagonalize all the covariant derivative D^μ $(\mu = 1,2,3,4)$ simultaneously, but only one of them can be diagonalized. For example, the eigen-mode expansion of D_4 keeps gauge covariance and is rather interesting, but this type of the expansion inevitably breaks the Lorentz covariance. Then, we consider the eigen-mode expansion of the Dirac operator $\not{D} = \gamma^\mu D^\mu$ or $D^2 = D^\mu D^\mu$, since such an expansion keeps both gauge symmetry and Lorentz covariance.

In particular, the Dirac-mode expansion is rather interesting because the Dirac operator $\not{D}$ directly connects with chiral symmetry breaking via the Banks-Casher relation [6] and its zero modes are related to the topological charge via the Atiyah-Singer index theorem [8]. Here, we mainly consider the manifestly gauge-invariant new method using the Dirac-mode expansion. Thus, the Dirac-mode expansion has some important merits.

- The Dirac-mode expansion method manifestly keeps both gauge and Lorentz invariance.
- Each QCD phenomenon can be directly investigated in terms of chiral symmetry breaking.

3.2 Confinement and Chiral Symmetry Breaking: Can we expect One-to-one Correspondence between them in QCD?

In particular, it is rather interesting and important to examine the correlation between confinement and chiral symmetry breaking [7, 9, 11, 15, 16], since the direct relation is not yet shown between them in QCD. The strong correlation between them has been suggested by the simultaneous phase transitions of deconfinement and chiral restoration in lattice QCD both at finite temperature [4] and in a small-volume box [4].

The close relation between confinement and chiral symmetry breaking has been also suggested in terms of the monopole/vortex degrees of freedom [9, 15, 16], which topologically appears in QCD by taking the maximally Abelian/center gauge [5, 17, 18]. For example, by removing the monopoles, confinement and chiral symmetry breaking are simultaneously lost in lattice QCD [15], as schematically shown in Fig.5. This indicates an important role of the monopole to both confinement and chiral symmetry breaking, and these two nonperturbative QCD phenomena seem to be related via the monopole.

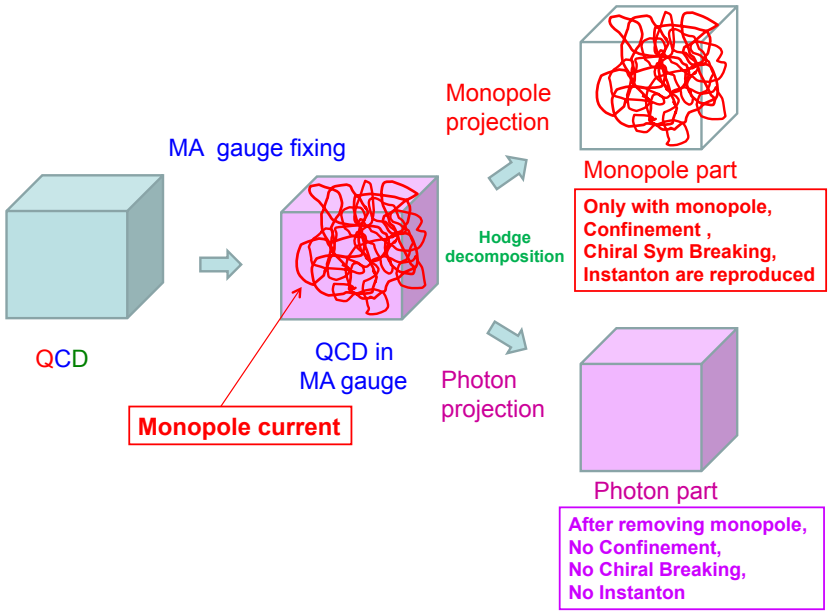

Figure 5: An illustration of the relevant role of monopoles to nonperturbative QCD. In the maximally Abelian gauge, QCD becomes Abelian-like due to the large off-diagonal gluon mass of about 1GeV [19], and there appears a global network of the monopole current [17, 18]. By the Hodge decomposition, the QCD system can be divided into the monopole part and the photon part. The monopole part has confinement [18], chiral symmetry breaking [15] and instantons [20], while the photon part does not have all of them.

However, as a possibility, removing the monopoles may be "too fatal" for most nonperturbative properties. If this is the case, nonperturbative QCD phenomena are simultaneously lost by their cut.

In fact, *if only the relevant ingredient of chiral symmetry breaking is carefully removed, how will be confinement?* To get the answer, we perform a direct investigation between confinement and chiral symmetry breaking, using the Dirac-mode expansion.

3.3 Eigen-mode of Dirac Operator in Lattice QCD

In lattice QCD with spacing a, the Dirac operator $\not{D} = \gamma_\mu D_\mu$ is expressed with $U_\mu(x)$ as

$$\not{D}_{x,y} \equiv \frac{1}{2a}\sum_{\mu=1}^{4}\gamma_\mu\left[U_\mu(x)\delta_{x+\hat{\mu},y} - U_{-\mu}(x)\delta_{x-\hat{\mu},y}\right], \tag{3.1}$$

where $U_{-\mu}(x) \equiv U_\mu^\dagger(x-\hat{\mu})$. In the use of hermite γ-matrix $\gamma_\mu^\dagger = \gamma_\mu$, $\not{D}$ is anti-hermite and satisfies $\not{D}_{y,x}^\dagger = -\not{D}_{x,y}$. The normalized eigen-state $|n\rangle$ of the Dirac operator $\not{D}$ is introduced as

$$\not{D}|n\rangle = i\lambda_n|n\rangle \tag{3.2}$$

with $\lambda_n \in \mathbf{R}$. Because of $\{\gamma_5, \not{D}\} = 0$, the state $\gamma_5|n\rangle$ is also an eigen-state of $\not{D}$ with the eigenvalue $-i\lambda_n$. The Dirac eigenfunction $\psi_n(x) \equiv \langle x|n\rangle$ obeys $\not{D}\psi_n(x) = i\lambda_n\psi_n(x)$, and its explicit form of the eigenvalue equation in lattice QCD is

$$\frac{1}{2a}\sum_{\mu=1}^{4}\gamma_\mu[U_\mu(x)\psi_n(x+\hat{\mu}) - U_{-\mu}(x)\psi_n(x-\hat{\mu})] = i\lambda_n\psi_n(x). \tag{3.3}$$

The Dirac eigenfunction $\psi_n(x)$ can be numerically obtained in lattice QCD, besides a phase factor.

According to $U_\mu(x) \to V(x)U_\mu(x)V^\dagger(x+\hat{\mu})$, the gauge transformation of $\psi_n(x)$ is found to be

$$\psi_n(x) \to V(x)\psi_n(x), \tag{3.4}$$

which is the same as that of the quark field. To be strict, for the Dirac eigenfunction, there can appear an irrelevant n-dependent global phase factor as $e^{i\varphi_n[V]}$, according to the arbitrariness of the definition of $\psi_n(x)$.

Note that the quark condensate $\langle\bar{q}q\rangle$, the order parameter of chiral symmetry breaking, is given by the zero-eigenvalue density $\rho(0)$ of the Dirac operator, via the Banks-Casher relation [6],

$$\langle\bar{q}q\rangle = -\lim_{m\to 0}\lim_{V\to\infty}\pi\rho(0). \tag{3.5}$$

Here, $\rho(\lambda) \equiv \frac{1}{V}\sum_n\langle\delta(\lambda-\lambda_n)\rangle$ is the spectral density of the Dirac operator. Also, the zero-mode number asymmetry of the Dirac operator $\not{D}$ is equal to the topological charge (the instanton number) $Q \equiv \frac{g^2}{16\pi^2}\int d^4x\,\mathrm{Tr}\,(G_{\mu\nu}\tilde{G}_{\mu\nu})$, which is known as the Atiyah-Singer index theorem, Index($\not{D}$)=Q [8].

3.4 Operator Formalism in Lattice QCD

To keep the gauge symmetry, careful treatments are necessary, since naive approximations may break the gauge symmetry. Here, we take the "operator formalism", as explained below.

We define the link-variable operator $\hat{U}_\mu$ by the matrix element of

$$\langle x|\hat{U}_\mu|y\rangle = U_\mu(x)\delta_{x+\hat{\mu},y}. \tag{3.6}$$

The Wilson-loop operator $\hat{W}$ is defined as the product of $\hat{U}_\mu$ along a rectangular loop,

$$\hat{W} \equiv \prod_{k=1}^{N}\hat{U}_{\mu_k} = \hat{U}_{\mu_1}\hat{U}_{\mu_2}\cdots\hat{U}_{\mu_N}. \tag{3.7}$$

For arbitrary loops, one finds $\sum_{k=1}^{N}\hat{\mu}_k = 0$. We note that the functional trace of the Wilson-loop operator $\hat{W}$ is proportional to the ordinary vacuum expectation value $\langle W\rangle$ of the Wilson loop:

$$\begin{aligned}
\mathrm{Tr}\,\hat{W} &= \mathrm{tr}\sum_x \langle x|\hat{W}|x\rangle = \mathrm{tr}\sum_x \langle x|\hat{U}_{\mu_1}\hat{U}_{\mu_2}\cdots\hat{U}_{\mu_N}|x\rangle \\
&= \mathrm{tr}\sum_{x_1,x_2,\cdots,x_N} \langle x_1|\hat{U}_{\mu_1}|x_2\rangle\langle x_2|\hat{U}_{\mu_2}|x_3\rangle\langle x_3|\hat{U}_{\mu_3}|x_4\rangle\cdots\langle x_N|\hat{U}_{\mu_N}|x_1\rangle \\
&= \mathrm{tr}\sum_x \langle x|\hat{U}_{\mu_1}|x+\hat{\mu}_1\rangle\langle x+\hat{\mu}_1|\hat{U}_{\mu_2}|x+\sum_{k=1}^{2}\hat{\mu}_k\rangle\cdots\langle x+\sum_{k=1}^{N}|\hat{U}_{\mu_N}|x\rangle \\
&= \sum_x \mathrm{tr}\{U_{\mu_1}(x)U_{\mu_2}(x+\hat{\mu}_1)U_{\mu_3}(x+\sum_{k=1}^{2}\hat{\mu}_k)\cdots U_{\mu_N}(x+\sum_{k=1}^{N}\hat{\mu}_k)\} \\
&= \langle W\rangle\cdot\mathrm{Tr}\,1. \qquad (3.8)
\end{aligned}$$

Here, "Tr" denotes the functional trace, and "tr" the trace over SU(3) color index.

The Dirac-mode matrix element of the link-variable operator $\hat{U}_\mu$ can be expressed with $\psi_n(x)$:

$$\langle m|\hat{U}|n\rangle = \sum_x \langle m|x\rangle\langle x|\hat{U}_\mu|x+\hat{\mu}\rangle\langle x+\hat{\mu}|n\rangle = \sum_x \psi_m^\dagger(x)U_\mu(x)\psi_n(x+\hat{\mu}). \qquad (3.9)$$

Although the total number of the matrix element is very huge, the matrix element is calculable and gauge invariant, apart from an irrelevant phase factor. Using the gauge transformation (3.4), we find the gauge transformation of the matrix element as

$$\begin{aligned}
\langle m|\hat{U}_\mu|n\rangle &= \sum_x \psi_m^\dagger(x)U_\mu(x)\psi_n(x+\hat{\mu}) \\
&\to \sum_x \psi_m^\dagger(x)V^\dagger(x)\cdot V(x)U_\mu(x)V^\dagger(x+\hat{\mu})\cdot V(x+\hat{\mu})\psi_n(x+\hat{\mu}) \\
&= \sum_x \psi_m^\dagger(x)U_\mu(x)\psi_n(x+\hat{\mu}) = \langle m|\hat{U}_\mu|n\rangle. \qquad (3.10)
\end{aligned}$$

To be strict, there appears an n-dependent global phase factor, corresponding to the arbitrariness of the phase in the basis $|n\rangle$. However, this phase factor cancels as $e^{-i\varphi_n}e^{i\varphi_n}=1$ between $|n\rangle$ and $\langle n|$, and does not appear for QCD physical quantities including the Wilson loop.

3.5 Dirac-mode Expansion and Projection

From the completeness of the Dirac-mode basis, $\sum_n |n\rangle\langle n| = 1$, we get $\hat{O} = \sum_m\sum_n |m\rangle\langle m|\hat{O}|n\rangle\langle n|$ for arbitrary operators. Based on this relation, the Dirac-mode expansion and projection can be defined. We define the projection operator $\hat{P}$ which restricts the Dirac-mode space,

$$\hat{P} \equiv \sum_{n\in A} |n\rangle\langle n|, \qquad (3.11)$$

where A denotes arbitrary set of Dirac modes. In $\hat{P}$, the arbitrary phase cancels between $|n\rangle$ and $\langle n|$. One finds $\hat{P}^2 = \hat{P}$ and $\hat{P}^\dagger = \hat{P}$. The typical projections are IR-cut and UV-cut of the Dirac modes:

$$\hat{P}_{\mathrm{IR}} \equiv \sum_{|\lambda_n|\geq\Lambda_{\mathrm{IR}}} |n\rangle\langle n|, \qquad \hat{P}_{\mathrm{UV}} \equiv \sum_{|\lambda_n|\leq\Lambda_{\mathrm{UV}}} |n\rangle\langle n|. \qquad (3.12)$$

Using the projection operator $\hat{P}$, we define the Dirac-mode projected link-variable operator,

$$\hat{U}_\mu^P \equiv \hat{P}\hat{U}_\mu\hat{P} = \sum_{m\in A}\sum_{n\in A}|m\rangle\langle m|\hat{U}_\mu|n\rangle\langle n|. \tag{3.13}$$

During this projection, there appears some nonlocality in general, but it would not be important for the argument of large-distance properties such as confinement. From the Wilson-loop operator $\hat{W} \equiv \prod_{k=1}^N \hat{U}_{\mu_k}$, we define the Dirac-mode projected Wilson-loop operator,

$$\begin{aligned}\hat{W}^P &\equiv \prod_{k=1}^N \hat{U}_{\mu_k}^P = \hat{U}_{\mu_1}^P\hat{U}_{\mu_2}^P\cdots\hat{U}_{\mu_N}^P = \hat{P}\hat{U}_{\mu_1}\hat{P}\hat{U}_{\mu_2}\hat{P}\cdots\hat{P}\hat{U}_{\mu_N}\hat{P} \\ &= \sum_{n_1,n_2,\cdots,n_{N+1}\in A}|n_1\rangle\langle n_1|\hat{U}_{\mu_1}|n_2\rangle\langle n_2|\hat{U}_{\mu_2}|n_3\rangle\cdots\langle n_N|\hat{U}_{\mu_N}|n_{N+1}\rangle\langle n_{N+1}|. \end{aligned}\tag{3.14}$$

Then, we obtain the functional trace of the Dirac-mode projected Wilson-loop operator,

$$\begin{aligned}\mathrm{Tr}\,\hat{W}^P &= \mathrm{Tr}\prod_{k=1}^N \hat{U}_{\mu_k}^P = \mathrm{Tr}\,\hat{U}_{\mu_1}^P\hat{U}_{\mu_2}^P\cdots\hat{U}_{\mu_N}^P = \mathrm{Tr}\,\hat{P}\hat{U}_{\mu_1}\hat{P}\hat{U}_{\mu_2}\hat{P}\cdots\hat{P}\hat{U}_{\mu_N}\hat{P} \\ &= \mathrm{tr}\sum_{n_1,n_2,\cdots,n_N\in A}\langle n_1|\hat{U}_{\mu_1}|n_2\rangle\langle n_2|\hat{U}_{\mu_2}|n_3\rangle\cdots\langle n_N|\hat{U}_{\mu_N}|n_1\rangle, \end{aligned}\tag{3.15}$$

which is manifestly gauge invariant. Here, the arbitrary phase factor cancels between $|n_k\rangle$ and $\langle n_k|$. Its gauge invariance is also numerically checked in the lattice QCD Monte Carlo calculation.

From $\mathrm{Tr}\,\hat{W}^P(R,T)$ corresponding to the $R\times T$ rectangular loop, we define the Dirac-mode projected inter-quark potential,

$$V^P(R) \equiv -\lim_{T\to\infty}\frac{1}{T}\ln\{\mathrm{Tr}\,\hat{W}^P(R,T)\}, \tag{3.16}$$

which is also manifestly gauge-invariant. In the unprojected case of $\hat{P}=1$, the ordinary inter-quark potential is obtained apart from an irrelevant constant,

$$V(R) = -\lim_{T\to\infty}\frac{1}{T}\ln\{\mathrm{Tr}\,\hat{W}(R,T)\} = -\lim_{T\to\infty}\frac{1}{T}\ln\langle W(R,T)\rangle + \text{irrelevant const.}, \tag{3.17}$$

because of $\mathrm{Tr}\,\hat{W} = \langle W\rangle\cdot\mathrm{Tr}\,1$, as was derived in Eq.(3.8).

3.6 Analysis of Confinement in terms of Dirac Modes in QCD

We consider various projection space A in the Dirac-mode space, e.g., IR-cut or UV-cut of Dirac modes. With this Dirac-mode expansion and projection formalism, we calculate the Dirac-mode projected inter-quark potential $V^P(R)$ in a gauge-invariant manner. In particular, using IR-cut of the Dirac modes, we directly investigate the role of low-lying Dirac modes to confinement, since the low-lying modes are responsible to chiral symmetry breaking.

As a technical difficulty of this formalism, we have to deal with huge dimensional matrices and their products. Actually, the total matrix dimension of $\langle m|\hat{U}_\mu|n\rangle$ is (Dirac-mode number)^2. On the L^4 lattice, the Dirac-mode number is $L^4\times N_c\times 4$, which can be reduced to be about $L^4\times N_c$, using the Kogut-Susskind technique [2, 4]. Even for the projected operators, where the Dirac-mode

space is restricted, the matrix is generally still huge. At present, we use a small-size lattice in the actual lattice QCD calculation.

We use SU(3) lattice QCD at $\beta = 5.6$ (i.e., $a \simeq 0.25$fm) on 6^4 at the quenched level. We show in Fig.6(a) the spectral density $\rho(\lambda)$ of the QCD Dirac operator $\not{D}$. The chiral property of $\not{D}$ leads to $\rho(-\lambda) = \rho(\lambda)$. Figure 6(b) is the IR-cut Dirac spectral density $\rho_{\rm IR}(\lambda) \equiv \rho(\lambda)\theta(|\lambda| - \Lambda_{\rm IR})$ with the IR-cutoff $\Lambda_{\rm IR} = 0.5a^{-1} \simeq 0.4$GeV. By removing the low-lying Dirac modes, the chiral condensate is largely reduced as $\langle\bar{q}q\rangle_{\Lambda_{\rm IR}}/\langle\bar{q}q\rangle \simeq 0.02$ around the physical region of $m \simeq 5$MeV.

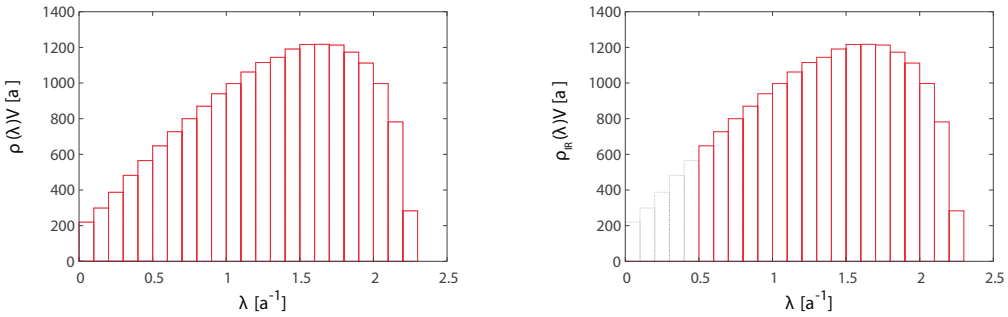

Figure 6: (a) The Dirac spectral density $\rho(\lambda)$ in lattice QCD at β=5.6 and 6^4. The volume V is multiplied. (b) The IR-cut Dirac spectral density $\rho_{\rm IR}(\lambda) \equiv \rho(\lambda)\theta(|\lambda| - \Lambda_{\rm IR})$ with the IR-cutoff $\Lambda_{\rm IR} = 0.5a^{-1} \simeq 0.4$GeV.

Figure 7 shows the inter-quark potential $V^P(R)$ after removing low-lying Dirac modes, which is obtained in lattice QCD with the IR-cut of $\rho_{\rm IR}(\lambda) \equiv \rho(\lambda)\theta(|\lambda| - \Lambda_{\rm IR})$ with the IR-cutoff $\Lambda_{\rm IR} = 0.5a^{-1}$. Remarkably, no significant change is observed on the inter-quark potential besides an irrelevant constant, that is, the confining force is almost unchanged, even after removing the low-lying Dirac modes, which are responsible to chiral symmetry breaking. This result indicates that one-to-one correspondence does not hold for confinement and chiral symmetry breaking in QCD.

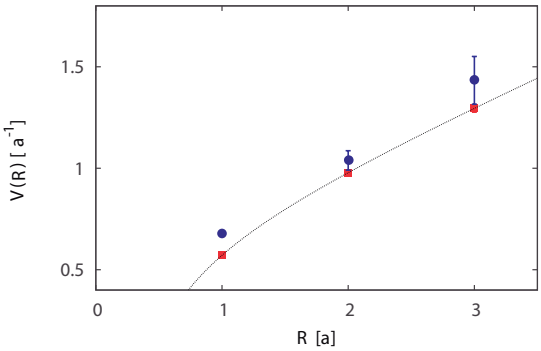

Figure 7: The circle symbol denotes the lattice QCD result of the inter-quark potential after removing low-lying Dirac modes, obtained with the IR-cut of $\rho_{\rm IR}(\lambda) \equiv \rho(\lambda)\theta(|\lambda| - \Lambda_{\rm IR})$ with the IR-cutoff $\Lambda_{\rm IR} = 0.5a^{-1}$. The square symbol denotes the original inter-quark potential. The potential is almost unchanged even after removing the low-lying Dirac modes, apart from an irrelevant constant.

We also investigate the UV-cut of Dirac modes in lattice QCD, and find that the confining force is almost unchanged by the UV-cut. This result seems consistent with the pioneering lattice study of Synatschke-Wipf-Langfeld [21]: they found that the confinement potential is almost reproduced

only with low-lying Dirac modes, using the spectral sum of the Polyakov loop [22]. Furthermore, we examine "intermediate-cut", where a certain part of $\Lambda_1 < |\lambda_n| < \Lambda_2$ of Dirac modes is removed, and obtain almost the same confining force. Then, we conjecture that the "seed" of confinement is distributed not only in low-lying Dirac modes but also in a wider region of the Dirac-mode space.

3.7 Discussions on "Confinement $\neq$ Chiral Symmetry Breaking" in QCD

Here, we discuss the obtained result of "confinement $\neq$ chiral symmetry breaking". As for their close relation via monopoles discussed in Sec.3.2, the monopole would be essential degrees of freedom for most nonperturbative QCD: confinement [18], chiral symmetry breaking [15], and instantons [20]. In fact, removing the monopole would be "too fatal" for the nonperturbative properties, so that nonperturbative QCD phenomena are simultaneously lost by their cut.

As shown in Fig.8, the Dirac zero-mode associated with an instanton is localized around it [8]. However, the localized objects are hard to contribute to the large-distance phenomenon of confinement, although such low-lying Dirac modes contribute to chiral symmetry breaking.

Recall that instantons contribute to chiral symmetry breaking, but do not directly lead to confinement [8]. Then, as a thought experiment, if only instantons can be carefully removed from the QCD vacuum, confinement properties would be almost unchanged, but the chiral condensate is largely reduced, and accordingly some low-lying Dirac modes disappear. Thus, in this case, confinement is almost unchanged, in spite of the large reduction of low-lying Dirac modes.

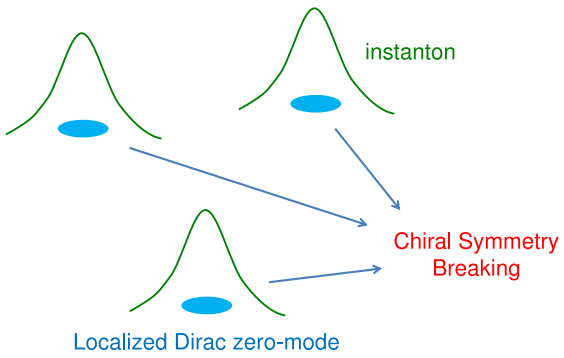

Figure 8: Around each instanton, the Dirac zero-mode is localized, and such low-lying Dirac modes contribute to chiral symmetry breaking. However, the localized objects are hard to contribute to confinement.

If their relation is not one-to-one, richer phase structure is expected in QCD. For example, the phase transition point can be different between deconfinement and chiral restoration in the presence of strong electro-magnetic fields, because of their nontrivial effect on chiral symmetry [23].

4. Summary and Concluding Remarks

First, we have studied the relevant gluon-momentum region for confinement in lattice QCD, based on the Fourier expansion. Remarkably, the string tension σ is almost unchanged even after removing the high-momentum gluon component above 1.5GeV in the Landau gauge. We then have concluded that confinement originates from the low-momentum gluon component below 1.5GeV, which is the upper limit to contribute to σ.

Second, we have developed a manifestly gauge-covariant expansion using the eigen-mode of the QCD Dirac operator $\not{D} = \gamma^\mu D^\mu$. With this method, we have performed a direct investigation of correspondence between confinement and chiral symmetry breaking in lattice QCD. As a remarkable fact, the confinement force is almost unchanged even after removing the low-lying Dirac modes, which are responsible to chiral symmetry breaking. This indicates that one-to-one correspondence does not hold for between confinement and chiral symmetry breaking in QCD.

Acknowledgements

H.S. thanks Profs. J.M. Cornwall, M. Creutz, J. Greensite, K. Langfeld, J. Papavassiliou, and E.T. Tomboulis for useful discussions and suggestions. He thanks the organizers of QCD-TNT II. H.S. is supported in part by the Grant for Scientific Research [(C) No. 23540306, Priority Arias "New Hadrons" (E01:21105006)] from the Ministry of Education, Culture, Science and Technology (MEXT) of Japan. The lattice QCD calculations are done on NEC SX-8R at Osaka University.

References

[1] Y. Nambu and G. Jona-Lasinio, *Phys. Rev.* **122** (1961) 345; *ibid.* **124** (1961) 246.

[2] K.G. Wilson, *Phys. Rev.* **D10** (1974) 2445; J.B. Kogut and L. Susskind, *Phys. Rev.* **D11** (1975) 395.

[3] M. Creutz, *Phys. Rev. Lett.* **43** (1979) 553; *Phys. Rev.* **D21** (1980) 2308.

[4] H.J. Rothe, *Lattice Gauge Theories*, World Scientific, 2005; M. Creutz, *Acta Phys. Slov.* **61** (2011) 1.

[5] Y. Nambu, *Phys. Rev.* **D10** (1974) 4262; G. 't Hooft, *Nucl. Phys.* **B190** (1981) 455.

[6] T. Banks and A. Casher, *Nucl. Phys.* **B169** (1980) 103.

[7] J.M. Cornwall, *Phys. Rev.* **D26** (1982) 1453; *Phys. Rev.* **D83** (2011) 076001.

[8] M. Shifman, *Instantons in Gauge Theories*, World Scientific, 1994, and its references.

[9] H. Suganuma, S. Sasaki, and H. Toki, *Nucl. Phys.* **B435** (1995) 207; *Prog. Theor. Phys.* **94** (1995) 373.

[10] E.T. Tomboulis, *PoS* (**LAT2009**) (2007) 336; *Mod. Phys. Lett.* **A24** (2009) 2717.

[11] A.C. Aguilar, D. Binosi, and J. Papavassiliou, *Phys. Rev.* **D78** (2008) 025010, and its references.

[12] A. Yamamoto and H. Suganuma, *Phys. Rev. Lett.* **101** (2008) 241601; *Phys. Rev.* **D79** (2009) 054504.

[13] T. Iritani *et al.*, *Phys. Rev.* **D80** (2009) 114505; *Phys. Rev.* **D83** (2011) 054502.

[14] A. Yamamoto and H. Suganuma, *Phys. Rev.* **D81** (2010) 014506; *PoS* (**LAT2010**) (2010) 294.

[15] O. Miyamura, *Phys. Lett.* **B353** (1995) 91; R.M. Woloshyn, *Phys. Rev.* **D51** (1995) 6411.

[16] R. Hollwieser, M. Faber, J. Greensite, U.M. Heller, and S. Olejnik, *Phys. Rev.* **D78** (2008) 054508.

[17] A.S. Kronfeld *et al.*, *Nucl. Phys.* **B293** (1987) 461; *Phys. Lett.* **B198** (1987) 516.

[18] J.D. Stack, S.D. Neiman, and R.J. Wensley, *Phys. Rev.* **D50** (1994) 3399.

[19] K. Amemiya and H. Suganuma, *Phys. Rev.* **D60** (1999) 114509.

[20] H. Suganuma, A. Tanaka, S. Sasaki, and O. Miyamura, *Nucl. Phys. Proc. Suppl.* **47** (1996) 302.

[21] F. Synatschke, A. Wipf, and K. Langfeld, *Phys. Rev.* **D77** (2008) 114018.

[22] C. Gattringer, *Phys. Rev. Lett.* **97** (2006) 032003; F. Bruckmann *et al.*, *Phys. Lett.* **B647** (2007) 56.

[23] H. Suganuma and T. Tatsumi, *Ann. Phys.* **208** (1991) 470; *Prog. Theor. Phys.* **90** (1993) 379.